REPORT DOCUMENTATION PAGE

Form Approved
OMB NO. 0704-0188

1. AGENCY USE ONLY (Leave Blank)	2. REPORT DATE	3. REPORT TYPE AND DATES COVERED
	03/15/2004	Final Progress Report 14 Jul 00 13 Apr 04

4. TITLE AND SUBTITLE
Study of Electron Relaxation Processes in Intersubband Laser heterostructures

5. FUNDING NUMBERS
DAAD 190010423

6. AUTHOR(S)
G. Belenky, M. Kisin, S. Suchalkin, S. Luryi

7. PERFORMING ORGANIZATION NAME(S) AND ADDRESS(ES)
The Research Foundation of State university of New York
Office of Research Services
Stony Brook, New York, 11794-3366

8. PERFORMING ORGANIZATION REPORT NUMBER

9. SPONSORING / MONITORING AGENCY NAME(S) AND ADDRESS(ES)
U. S. Army Research Office
P.O. Box 12211
Research Triangle Park, NC 27709-2211

10. SPONSORING / MONITORING AGENCY REPORT NUMBER
39792.14-EL

11. SUPPLEMENTARY NOTES
The views, opinions and/or findings contained in this report are those of the author(s) and should not be construed as an official Department of the Army position, policy or decision, unless so designated by other documentation.

12 a. DISTRIBUTION / AVAILABILITY STATEMENT
Approved for public release; distribution unlimited.

12 b. DISTRIBUTION CODE

13. ABSTRACT (Maximum 200 words)

Comprehensive experimental and theoretical study of the electron relaxation processes responsible for the depopulation of the lower lasing states in intersubband and interband laser heterostructures has been accomplished. In theory, LO-phonon assisted relaxation has been given special attention due to the high impact on the laser gain and temperature performance. We showed that in type-II laser heterostructures LO phonon assisted depopulation of the lower lasing states is more efficient than corresponding interband tunneling process. We suggested type-II intersubband laser design with phonon-assisted depopulation and lower lasing level located near the upper edge of the heterostructure leaky window, where direct interband tunneling depopulation is inefficient. This design is beneficial for the laser performance providing the highest value of the matrix element for intrawell optical lasing transition and simultaneously preventing thermal backfilling of the lower lasing states. We also proposed a piezo-acoustic DFB QCL tunable in a wide wavelength range, which is especially important for spectroscopic applications of the quantum cascade lasers. Experimental program was focused on the study of temperature dependence of the optical gain and loss which is the most important factors for laser high-temperature operation. Special measurement technique has been developed for MIR type-II lasers which allows gain and loss spectra analysis in wide temperature range. Heat removal and hole leakage processes were also studied using MQW InP-based laser and laser array heterostructures.

14. SUBJECT TERMS
Semiconductor lasers, Electron relaxation, Optical gain, Optical loss

15. NUMBER OF PAGES
10

16. PRICE CODE

17. SECURITY CLASSIFICATION OR REPORT	18. SECURITY CLASSIFICATION ON THIS PAGE	19. SECURITY CLASSIFICATION OF ABSTRACT	20. LIMITATION OF ABSTRACT
UNCLASSIFIED	**UNCLASSIFIED**	**UNCLASSIFIED**	**UL**

Statement of the Problem

The ability to engineer the composition of materials on an atomic scale gave rise to many novel optical devices, e. g. type-I quantum cascade (QC) lasers, type-II interband cascade (IC) and diode lasers, quaternary alloy based multiple quantum well (MQW) diode lasers, etc. Considerable progress has been made in the development of mid-infrared (MIR) laser sources, which are desirable for numerous military, security, and civilian applications including countermeasures, chemical sensing, and free space communications [1]. However, the most prominent laser design and even the optimum material system is not yet resolved issue for MIR range. Low cost, higher efficiency and reduced size favor electrically controlled semiconductor lasers, making them more preferable than optically pumped structures. As a result, there is especially strong demand for injection semiconductor lasers operating in MIR wavelength range and capable for continuous wave (CW) room temperature (RT) operation.

Present MIR injection lasers are still limited in their performance. InP and GaAs based type-I QC lasers suffer from inherently high nonradiative intersubband electron relaxation assisted by LO-phonon emission. This restrains the output optical power and affects the temperature performance of the laser [2]. CW operation of the InAs/GaSb based type-II lasers has been demonstrated only up to 195K for "W" diode lasers [3] and up to 214K for interband cascade lasers [4]. The enhancement of the temperature performance of these lasers is still very problematic due to lack of understanding of the basic relaxation mechanisms in type-II heterostructures, unknown main sources of the optical loss, and unsatisfactory thermal and transport properties of the laser structures. As of this time, MQW diode lasers based on quaternary alloys InGaAsSb/AlGaAsSb with traditional type-I band alignment demonstrate the best high-temperature CW characteristics yet in restricted wavelength region $\lambda < 3$ μm [5], which is determined both by material band-gap limitations and insufficient hole confinement and transport.

Design and improvement of modern semiconductor lasers can be accomplished only through extensive theoretical and experimental study of intra- and intersubband electron dynamics in semiconductor heterostructures leading to deep understanding of the heterostructure optical characteristics, such as the optical gain, optical loss, and α-factor spectra. This project includes a research program for all three basic types of MIR lasers

- Enhancement of the phonon-assisted depopulation of the lower lasing states in type-II interband and type-I intersubband cascade lasers. Study of the gain modulation in type-I DFB-QCL.
- Study of optical gain and loss and performance advances in type-II electrically pumped mid-infrared lasers. Enhancement of the laser temperature performance.
- Hole dynamics and heat removal management in MQW laser heterostructures.

Summary of the Results

Comprehensive theoretical study of the electron relaxation processes responsible for the depopulation of the lower lasing states in intersubband and interband laser heterostructures has been accomplished during this project [6]. LO-phonon assisted relaxation has been given special attention due to the high impact on the laser gain and temperature performance.

- An exact analytical representation was obtained for electron eigenstates in the full 8-band Kane model and applied to calculate the depopulation rate of the lower lasing state in active region of type-II intersubband cascade laser [7]. We showed that interband tunneling rate takes its maximum value when the depopulated states belong to the upper of the coupled electron- and hole-like subbands in the "leaky window" of the broken-gap type-II InAs/GaSb heterostructure.

- The rate of interband electron transitions assisted by LO-phonon emission was studied in an InAs/GaSb double quantum well heterostructure, which models the active region of a type-II intersubband cascade laser [8]. The rate of phonon assisted depopulation process was further compared with the interband tunneling rate through the leaky window. We showed that the phonon-assisted process can dominate over the elastic tunneling if the initial and final electron states anticross and the anticrossing gap is designed smaller than the LO-phonon energy.

- Detailed analysis of the electron-phonon resonance in type-II intersubband cascade laser in extended k-space was performed [9]. We found that the main peak of the electron-phonon resonance corresponds to electron transitions from the lowest electron-like subband to the top of the highest light-hole-like subband, which is strongly spin-split and displaced from the center of the Brillouin zone due to the asymmetry of the InAs/GaSb quantum well heterostructure.

- Electron-phonon wave function overlap was optimized for electron-phonon resonance in type-II heterostructures [10] and improved laser design with enhanced optical gain was suggested [11]. We showed that LO phonon assisted relaxation in type-II heterostructures is more efficient for the fast depopulation of the lower lasing states than the corresponding intersubband process in type-I double quantum well heterostructures. Phonon-assisted depopulation can be conveniently employed even when the lower lasing level is designed near the upper edge of the heterostructure leaky window, where direct interband tunneling depopulation becomes inefficient. This design is beneficial for the type-II laser performance providing the highest value of the matrix element for intrawell optical lasing transition and simultaneously preventing thermal backfilling of the lower lasing states.

- Periodic modulation of the carrier density and the optical gain, produced by a piezo-acoustic wave propagating along the optical axis of a unipolar QCL, was investigated [12]. We predict distributed feedback in such a piezo-DFB QCL sufficient for providing the mode suppression ratio over 30 dB [13]. In contrast to bipolar lasers, the piezoelectric modulation of unipolar carrier density in type-I QCL is not accompanied by a degradation of the average gain. We showed that the wavelength of the main DFB mode can be tuned in a wide range, which is especially important for spectroscopic applications of the quantum cascade lasers.

The program of experimental study of the laser heterostructures was focused on the understanding of the temperature dependence of the optical gain and loss which is of crucial importance for laser high-temperature operation [14]. Special measurement techniques have been developed for MIR type-II lasers which allow gain and loss spectra analysis in wide temperature range. Heat removal and hole leakage processes were also studied using MQW InP-based laser and laser array heterostructures.

- Lateral mode spatial filtering technique combined with the Hakki-Paoli approach was developed for gain measurements in broad area type II InAs/GaInSb mid-infrared diode lasers (λ=3-3.1μm) with W-type active region design [15]. We analyzed the internal optical loss obtained from the gain spectra and found that the optical loss of 18-20 cm^{-1} was the same for devices with either ten or five periods in active region. The optical loss is found to be nearly constant in such devices in wide temperature range between 80 and 160K. Analysis of the differential gain and spontaneous emission spectra shows that the main contribution to the temperature dependence of the threshold current is Auger recombination, which dominates the threshold current within almost the entire temperature range studied.

- A method of optical gain and loss measurement was developed for type-II InAs/GaInSb interband cascade MIR lasers operating in the 3.4-3.6 μm wavelength range [16]. The maximum temperature of CW operation was found to be limited by strong gain saturation due to active region overheating, while the temperature increase of the total optical loss was relatively small. In devices with a longer lasing wavelength and a thinner substrate-side cladding layer, a strong periodic modulation of the optical gain spectra was observed [17]. We showed that this modulation is consistent with the predicted effect of the resonant optical leakage into the substrate.

- A theoretical model for laser and laser array heating was developed and applied to heat removing analysis in one- and two-dimensional laser arrays [18]. A 20-element 1-cm-wide one-dimensional diode laser array mounted in a microchannel water–cooled heatsink revealed continuous-wave power of 25 W at 1.47-μm at the coolant temperature of 16 C. A two-dimensional array comprising four laser bars achieved a quasi-continuous-wave output of 110-W at a wavelength of

1.49 μm with an 8-9 nm full-width-half-maximum spectrum width. The coolant temperature was 18 C. Thermal resistances of 0.56, 0.4 and 0.34 K/W were experimentally and theoretically determined for arrays with fill factors of 10, 20 and 40 %, respectively.

- The temperature dependence of the performance of MQW lasers was analyzed using detailed microscopic simulations and compared to measurements [19]. Devices with different profiles of acceptor doping in the active region were experimentally studied [20]. Excellent agreement between measurement and simulation was achieved as a function of both temperature and doping profile for static and dynamic properties of the lasers, threshold current density and effective differential gain. We showed that the static carrier density, and hence the contribution to the optical gain, varies significantly from the quantum wells on the p-side of the active layer to those on the n-side. Furthermore, the modal differential gain and the carrier density modulation also vary. Both effects are a consequence of the carrier dynamics involved in transport through the MQW active layer. Despite the complexity of the dynamic response of the MQW laser, the resonance frequency is determined by an effective differential gain, which we show can be estimated by a gain weighted average of the local differential gain in each well. Direct measurement of lateral carrier leakage were carried out for MQW capped mesa buried heterostructure (CMBH) lasers with mesa width ranging from 1μm (standard single mode) to 100 μm (wide area) [21]. The structures were fabricated on one wafer with identical current blocking layers at the sides. Measurement of gain and loss in the devices showed that the single mode devices have 6-8 cm^{-1} higher loss and 40% lower optical confinement than the wide area devices. Beyond these differences, the measurements showed that up to 30% of the threshold current in the single mode CMBH lasers does not contribute to the pumping of the MQW active region. Injection efficiency is measured to be close to unity for both single mode and wide mesa devices. Scenarios to explain this parasitic current include the potential role for non-radiative recombination centers at the regrown epitaxial interface, which are consistent with all of the experimental results.

References

1. D. V. Donetsky, R. U. Martinelli, and G. L. Belenky, "Mid-infrared GaSb-based lasers with type-I heterointerfaces," in *Advanced Semiconductor Heterostructures: Novel Devices, Potential Device Applications and Basic Properties*, World Scientific, Singapore, pp. 87-100 (2003).
2. F. Capasso, C. Gmachl, D. L. Sivco, and A. Y. Cho, "Quantum cascade lasers," *Physics Today*, vol. 55, pp. 34-40 (2002).
3. W. W. Bewley, H. Lee, I. Vurgaftman, R. J. Menna, C. L. Felix, R. U. Martinelli, D. W. Stokes, D. Z. Garbuzov, J. R. Meyer, M. Maiorov, J. C. Connolly, A. R. Sugg, and G. H. Olsen, "Continuous-wave operation of λ=3.25 μm broadened-waveguide W quantum-well diode lasers up to T=195 K," *Appl. Phys. Let.*, vol. 76, pp. 256-258 (2000).
4. J. L. Bradshaw, N. P. Breznay, J. D. Bruno, J. M. Gomes, J. T. Pham, F. J. Towner, D. E. Wortman, R. L. Tober, C. J. Monroy, and K. A. Oliver, "Resent progress in the development of the type II interband cascade lasers," *Physica E*, vol. 20, pp. 479-485 (2004).
5. J. G. Kim, L. Shterengas, R. U. Martinelli, G. L. Belenky, D. Z. Garbuzov, and W. K. Chan, "Room-temperature 2.5 μm InGaAsSb/AlGaAsSb diode lasers emitting 1 W continuous waves," *Applied Physics Letters*, vol. 81, pp. 3146-3148 (2002).
6. M.V. Kisin, M. Dutta and M. A. Stroscio, “Eectron-phonon interactions in intersubband laser heterostructures”, in *Advanced Semiconductor Heterostructures: Novel Devices, Potential Device Applications and Basic Properties*, Selected Topics in Electronics and Systems - Vol. 28, World Scientific, Singapore pp. 1-30 (2003); also in *International Journal of High Speed Electronics and Systems*, vol. 12, No. 4, pp. 939-968 (2002).
7. M.V. Kisin, M.A. Stroscio, S. Luryi, G. Belenky. “Interband tunneling depopulation in InAs/GaSb type-II cascade laser heterostructure”. *Physica E*, vol. 10, No 4, pp. 576-586 (2001).
8. M.V. Kisin, M.A. Stroscio, G. Belenky, S. Luryi. “Interband Phonon-Assisted Tunneling in InAs/GaSb Heterostructures”. *Physica B*, vol. 316-317, pp. 223-225 (2002).
9. M.V. Kisin, M.A. Stroscio, G. Belenky, S. Luryi. “Electron-Phonon Resonance in InAs/GaSb type-II Laser Heterostructures”. *Appl. Phys. Lett.*, vol. 80, No 12, 2174-2176 (2002); also in Virtual Journal of Nanoscale Science & Technology vol. 5, Issue 13 (2002).
10. M. V. Kisin, M. A. Stroscio, G. Belenky, S. Luryi “Resonant phonon-assisted depopulation in type-I and type-II intersubband laser heterostructures”, *Institute of Physics Conference Series*, No 174, pp. 443-446 (2003).

11. M.V. Kisin, G. Belenky, S. Luriy, "Enhancement of the Phonon Depopulation in Intersubband Cascade Lasers". *International Workshop on Quantum Cascade Lasers*, January 4-8, 2004, Sevelle, Spain.

12. M. V. Kisin and S. Luryi, "Piezoacoustic modulation of gain and distributed feedback for quantum cascade lasers with widely tunable emission wavelength", *Appl. Phys. Lett.* vol. 82, No 6, 847-849 (2003).

13. S. Luriy, M.V. Kisin. "Distributed Feedback Quantum Cascade Laser with Widely Tunable Wavelength". *International Workshop on Quantum Cascade Lasers*, January 4-8, 2004, Sevelle, Spain.

14. G. Belenky, L. Shterengas, C.W. Trussell, C.L. Reynolds, Jr., M.S. Hybertsen, R. Menna, Trends in semiconductor laser design: Balance between leakage, gain and loss in InGaAsP/InP MQW structures, in *Future Trends in Microelectronics: The Nano-Millennium*, Wiley, New York, pp.231-241, (2002).

15. S. Suchalkin, D. Westerfeld, D. Donetski, S. Luryi, G. Belenky, R. Martinelli, I. Vurgaftman, and J. Meyer. "Optical gain and loss in 3 μm diode W quantum-well lasers", *Appl. Phys. Lett*. vol. 80, No 16. pp 2833-2835 (2002).

16. S. Suchalkin, J. Bruno, R. Tober, D. Westerfeld, M. Kisin, G. Belenky, "Experimental study of the optical gain and loss in InAs/GaInSb interband cascade lasers," *Appl. Phys. Let.*, vol. 83, No 8, pp. 1500-1502 (2003).

17. D. Westerfeld, S. Suchalkin, M. Kisin, G. Belenky, J. Bruno, R. Tober, "Experimental study of optical gain and loss in 3.4-3.6 μm interband cascade lasers,"*IEE Proc.-Optoelectron.*, vol. 150, No 4, pp. 293-297 (2003).

18. Gourevitch, G. Belenky, D. Donetsky, B. Laikhtman, D.Westerfeld, C.W. Trussell, H. An, Z. Shellenbarger, and R. Martinelli, "1.47-1.49 μm InGaAsP-InP Diode Laser Arrays", *Appl. Phys. Let.*, vol. 83, No4, pp. 617-619 (2003).

19. Witzigmann, M. S. Hybertsen, C. L. Reynolds, G. L. Belenky, L. Shterengas, and G. E. Shtengel, "Dependence of Static and Dynamic 1.3μm Multi-Quantum-Well Laser Microscopic Simulation of the Temperature Performance", *IEEE Journal of Quantum Electronics*, vol 39, No 1, pp. 120-129 (2003).

20. G. Belenky, C.L. Reynolds Jr., L. Shterengas, M.S. Hybertsen, D.V. Donetsky, G.E. Stengel, S. Luryi, "Effect of p-doping on the temperature dependence of differential gain in FP and DFB 1.3 μm InGaAsP-InP multiple-quantum well lasers", *IEEE Photonics Technology Letters*, vol. 12, No 8, pp. 969-971 (2000).

21. G. Belenky, L. Shterengas, C.L. Reynolds Jr., M.W. Focht, M.S. Hybertsen, B. Witzigmann, "Direct measurement of lateral carrier leakage in 1.3μm InGaAsP MQW capped mesa buried heterostructure lasers", *IEEE Journal of Quantum Electronics*, vol. 38, No 9, pp. 1276-1281 (2002).

List of Publications supported under this Contract

Papers published in peer-reviewed journals:

1. D. Westerfeld, S. Suchalkin, M.V. Kisin, G. Belenky, J. Bruno, R. Tober, "Experimental study of optical gain and loss in 3.4-3.6 μm interband cascade lasers,"*IEE Proc.-Optoelectron.*, vol. 150, No 4, pp. 293-297 (2003).
2. S. Suchalkin, D. Westerfeld, D. Donetski, S. Luryi, G. Belenky, R.Martinelli, I. Vurgaftman, and J. Meyer. "Optical gain and loss in 3 μm diode W quantum-well lasers", *Appl. Phys. Lett*. vol. 80, No 16. 2833-2835 (2002).
3. S. Suchalkin, J. Bruno, R. Tober, D. Westerfeld, M. Kisin, G. Belenky, "Experimental study of the optical gain and loss in InAs/GaInSb interband cascade lasers," *Appl. Phys. Let.*, vol. 83, No 8, pp. 1500-1502 (2003).
4. M.V. Kisin, M. Dutta and M. A. Stroscio, "Eectron-phonon interactions in intersubband laser heterostructures", in *Advanced Semiconductor Heterostructures: Novel Devices, Potential Device Applications and Basic Properties*, Selected Topics in Electronics and Systems - Vol. 28, World Scientific, Singapore (2003); also in *International Journal of High Speed Electronics and Systems*, vol. 12, No. 4, 939-968 (2002).
5. M.V. Kisin, M.A. Stroscio, G. Belenky, S. Luryi. "Electron-Phonon Resonance in InAs/GaSb type-II Laser Heterostructures". *Appl. Phys. Lett*. vol. 80, No 12, 2174-2176 (2002)
6. M. V. Kisin, M. A. Stroscio, G. Belenky, S. Luryi "Resonant phonon-assisted depopulation in type-I and type-II intersubband laser heterostructures", *Institute of Physics Conference Series*, No 174, pp. 443-446 (2003).
7. M.V. Kisin, M.A. Stroscio, G. Belenky, S. Luryi. "Interband Phonon-Assisted Tunneling in InAs/GaSb Heterostructures". *Physica B*, vol. 316-317, pp. 223-225 (2002).
8. M.V. Kisin, M.A. Stroscio, S. Luryi, G. Belenky. "Interband tunneling depopulation in InAs/GaSb type-II cascade laser heterostructure". *Physica E*, vol. 10, No 4, pp. 576-586 (2001).
9. G. Belenky, L. Shterengas, C.W. Trussell, C.L. Reynolds, Jr., M.S. Hybertsen, R. Menna, Trends in semiconductor laser design: Balance between leakage,gain and loss in InGaAsP/InP MQW structures, in *Future Trends in Microelectronics: The Nano-Millennium*, p.231-241, Wiley (2002).
10. A. Gourevitch, G. Belenky, D. Donetsky, B. Laikhtman, D.Westerfeld, C. W. Trussell, H. An, Z. Shellenbarger, and R. Martinelli, "1.47-1.49 μm InGaAsP-InP Diode Laser Arrays", *Appl. Phys. Lett*. vol. 83, No4, 617-619 (2003).

11. B. Witzigmann, M. S. Hybertsen, C. L. Reynolds, G. L. Belenky, L. Shterengas and G. E. Shtengel, "Dependence of Static and Dynamic 1.3 μm Multi-Quantum-Well Laser Microscopic Simulation of the Temperature Performance", *IEEE Journal of Quantum Electronics*, vol 39, No 1, 120-129 (2003).

12. G. Belenky, L. Shterengas, C.L. Reynolds Jr., M.W. Focht, M.S. Hybertsen, B. Witzigmann, "Direct measurement of lateral carrier leakage in 1.3μm InGaAsP MQW capped mesa buried heterostructure lasers", *IEEE Journal of Quantum Electronics*, vol. 38, No 9, 1276-1281 (2002).

13. G. Belenky, C.L. Reynolds Jr., L. Shterengas, M.S. Hybertsen, D.V. Donetsky, G.E. Stengel, S. Luryi, "Effect of p-doping on the temperature dependence of differential gain in FP and DFB 1.3 μm InGaAsP-InP multiple-quantum well lasers", *IEEE Photonics Technology Letters*, vol. 12, No 8, 969-971 (2000).

Papers published in conference proceedings:

1. S. Suchalkin, D. Westerfeld, D. Donetski, R. Martinelli, I.Vurgaftman, J. Meyer, S.Luryi, and G. Belenky. "Optical gain and loss in 3 μm diode ``W'' quantum-well lasers", in *Novel In-Plane Semiconductor Lasers*, 21-23 January 2002, San Jose, CA, USA; *Proceedings of SPIE*, vol. 4651, p. 185 (2002).

2. M.V. Kisin, M. A. Stroscio, G. Belenky, S. Luryi. "Intersubband Phonon Assisted Transitions in type-II InAs-GaSb Heterostructures", in *Proceedings of the Sixth International Conference on Intersubband Transitions in Quantum Wells*, ITQW'01, 10-14 September 2001, Asilomar, California, USA.

3. M.V. Kisin, M. A. Stroscio, G. Belenky, S. Luryi. "Interband Phonon Assisted Tunneling in InAs-GaSb Heterostructures", in *Proceedings of the Tenth International Conference on Phonon Scattering in Condensed Matter*, Phonons'01, 12-17 August 2001, Dartmouth College, Hanover, New Hampshire, USA.

List of Scientific Personnel

Gregory Belenky, Professor.

Serge Luryi, Professor.

Mikhail Kisin, Research Professor.

Sergey Suchalkin, Research Scientist.

David Westerfeld, PhD student.

Leon Shterengas, PhD student.

Reports of Inventions

None

Experimental study of optical gain and loss in 3.4–3.6 μm interband cascade lasers

D. Westerfeld, S. Suchalkin, M. Kisin, G. Belenky, J. Bruno and R. Tober

Abstract: The optical gain and loss of lasers operating over the wavelength range of 3.4 to 3.6 μm were measured using the Hakki–Paoli technique. The optical loss was found to increase with increasing temperature, from 38 cm^{-1} at 80 K to 62 cm^{-1} at 200 K for a typical sample. Above the maximum continuous-wave (CW) lasing temperature, the modal gain was observed to saturate before the device reached threshold. The reason for the gain saturation is the active area overheating in the CW mode. Some of the samples exhibited strong mode-grouping effects. These effects indicate the presence of 'leaky modes' in these structures and lead to a significant reduction of net gain at certain frequencies.

Introduction

The interband cascade laser (ICL) has great potential to meet the commercial and military demand for an efficient, compact, reliable and low cost mid-IR source. In the eight years since these devices were first suggested [1] many of their theoretical advantages have already been demonstrated. Various devices have demonstrated high performance, including output powers of 6 W/facet, threshold currents of 13.1 A/cm^2, room-temperature pulsed operation [2], and record high-power conversion efficiencies for mid-IR diode lasers of 18% [3].

Despite encouraging theoretical predictions [4], ICLs have not yet demonstrated room temperature continuous-wave (CW) operation. Since CW operation at or near room temperature is required for many potential applications, it is important to understand the factors limiting ICL high-temperature performance.

The temperature dependence of optical gain and loss are therefore of great interest. Loss measurements using the inverse cavity-length method are complicated by the extreme variability in the device-to-device characteristics of these lasers [2], and very little data has been published. The Hakki–Paoli method of determining optical gain and loss, employed in this work, has the advantage of requiring only one sample to determine both optical gain and loss.

Some of the samples studied exhibited strong mode grouping, as evidenced by periodic distortions in the gain curve. This effect can be ascribed to mode leakage into the substrate, which contributes an additional wavelength-dependent optical loss in some of the devices investigated.

IEE Proceedings online no. 20030539

doi: 10.1049/ip-opt:20030539

Paper received 12th November 2002

D. Westerfeld, S. Suchalkin, M. Kisin and G. Belenky are with the Electrical Engineering Department, Light Engineering Building, State University of New York at Stony Brook, Stony Brook, New York 11794, USA

J. Bruno is with Maxion Technologies Inc., Hyattsville, Maryland 20782-2003, USA

R. Tober is with the Army Research Laboratory, Adelphi, Maryland 20873-1197, USA

2 Experiment

The interband cascade lasers (ICLs) used in this experiment contained 18 stages of AlSb/InAs/GaInSb/InAs/AlSb asymmetric 'W' quantum wells. The active quantum wells were separated by n-type injection regions consisting of AlInSb, InAs and AlSb layers. InAs/AlSb superlattices were used for top and bottom cladding layers. The devices were grown by molecular beam epitaxy on wafers of p-type GaSb. Broad-area mesa-stripe lasers were formed by etching and cleaving the wafers to form samples with cavity lengths near 0.5 mm. The facets were left uncoated. Devices were mounted epi-layer side up on copper heatsinks and electrically connected by wire bonding. Finished lasers were mounted on the temperature-regulated cold finger of a nitrogen cryostat.

The samples came from two different wafers with slightly different designs. One set of samples lased near 3.4 μm, whereas slight differences in the details of the active region caused the other set to lase at a slightly longer 3.6 μm. Additionally, there were very minor differences in the thickness of the cladding layers between the two sets of devices. The 3.4 μm samples had mesa widths of 65 or 115 μm, whereas the 3.6 μm samples had mesa widths of 60 μm or 110 μm.

The Hakki–Paoli technique [5] determines the gain and optical loss of a particular lateral laser mode by analysing the contrast between the peaks and valleys of the Fabry–Perot fringes in the laser's sub-threshold amplified spontaneous emission (ASE) spectrum. The broad area devices used in this investigation are able to support many lateral modes, and so the ASE consists of a superposition of contributions from all of the cavity modes.

In order to apply the Hakki–Paoli technique, it is necessary to separate the lateral modes so that the Fabry–Perot fringes of a small set of lateral modes can be clearly resolved. In this study, the lateral modes were separated using spatial filtering [6] of the laser's far-field emission. The lasers were placed ~1 m from a Nicolet Nexus 670 Fourier transform infrared (FTIR) spectrometer, and a cylindrical lens was used to provide fast axis collimation of the ASE. By careful positioning of the sample relative to the

spectrometer, high-contrast spectra were obtained. This simple method of spatial filtering compared favourably to a more complex imaging technique using a reflective objective and movable diaphragm. Adding a polariser into the optical path did not increase the ASE contrast.

3 Results

3.1 Internal loss

3.1.1 Temperature dependence: A typical mode-separated ASE spectrum obtained under continuous wave (CW) operation is shown in Fig. 1. The device gain was computed from multiple ASE spectra obtained at different injection currents, resulting in the curves of Fig. 2. The vertical axis on this curve (and those to follow) is the modal gain minus optical losses or net gain. With this convention, zero on the vertical axis corresponds to threshold.

The total cavity loss can be estimated by the low energy saturation of the gain curves. For the example given, the total optical loss is approximately 53 cm^{-1}. There is considerable uncertainty in determining the loss due to the decrease of the signal to noise ratio at the low energy edge of the spectrum. This contributes to a roughly estimated uncertainty in the loss of the order of $\pm 5\,cm^{-1}$.

The total loss is the sum of the internal loss α_i, and the mirror loss α_m. We used the known cavity length, L, and the observed spacing of the Fabry–Perot fringes to determine the effective index of the cavity. From the index, we determined the mirror reflectivity, R. The mirror loss was then determined using $\alpha_m = \ln(1/R)/L$. The mirror loss for all of these samples was 22 cm^{-1}.

After subtracting the mirror loss, we found the internal loss for the 3.4 μm, 65 μm mesa device of Fig. 2 to be approximately 31 cm^{-1} at a heatsink temperature of 80 K. The internal loss for the 3.4 μm, 115 μm mesa device at 80 K was somewhat lower at 19 cm^{-1}. The internal loss for a 3.6 μm wavelength, 110 μm mesa width sample was 38 cm^{-1} at 80 K.

The temperature dependence of the internal loss was measured, and a plot is shown in Fig. 3. The internal loss increased from 38 cm^{-1} at a heatsink temperature of 80 K to 62 cm^{-1} at 200 K. At least part of the increased loss at higher temperatures can be explained by higher free carrier absorption due to the higher pump currents at the higher temperatures.

3.1.2 Wavelength dependence: The 3.6 μm lasers produced very unusual ASE spectra with periodic modulation, as shown in the inset of Fig. 4. This mode grouping effect has been explained [7, 8] by an additional periodic cavity loss caused by mode leakage that arises when the refractive index of the substrate is close to the index of the waveguide, the substrate is transparent and the optical mode confinement is poor. In this case, light that escapes from the waveguide is able to establish standing waves in the substrate.

The net gain computed from the ASE spectrum shown in the inset of Fig. 4 is depicted as the lower curve in Fig. 4. The peaks in the gain spectrum occur when the substrate modes are not resonant with the waveguide modes. At the peaks, very little energy is lost to the substrate modes, and so there is very little additional loss due to the mode leakage. For this reason, a curve drawn by connecting the peaks on Fig. 4 resembles the gain curves for the devices that do not exhibit this leaky mode effect (e.g. Fig. 2). A curve drawn in this way can be used to estimate the waveguide losses for these leaking devices by using the low energy saturation, as discussed earlier.

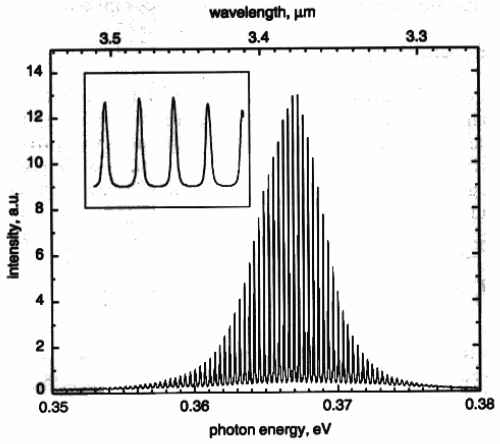

Fig. 1 *Continuous-wave amplified spontaneous emission spectrum at 80 K for a 0.5 mm-long device with a 115 μm mesa*
The inset shows the Fabry–Perot modes in greater detail

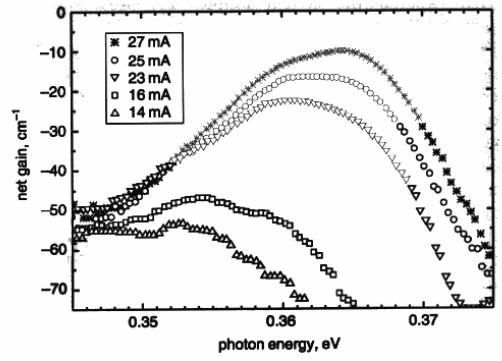

Fig. 2 *Net gain against energy under different injection currents for a 3.4 μm device with a 65 μm mesa width at 80 K*
Zero on the vertical axis corresponds to threshold

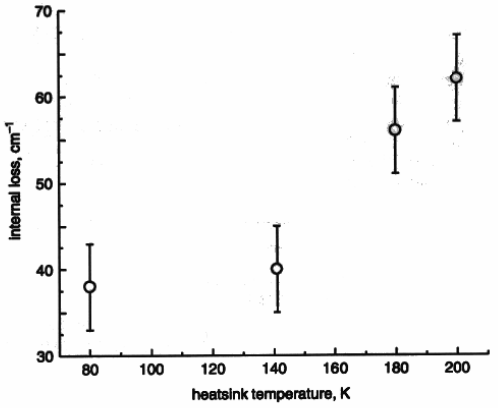

Fig. 3 *Variation of internal loss with heatsink temperature for a 3.4 μm, 65 μm mesa device*

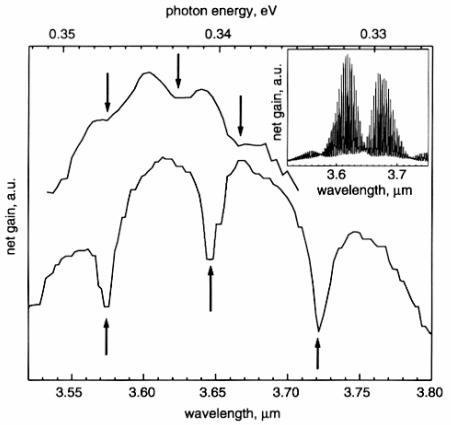

Fig. 4 *Net gain against energy for two 3.6 μm wavelength devices*

Top trace: 130 μm substrate thickness
Bottom trace: 75 μm substrate thickness
The spacing of the minima changes in accordance with theory
Inset: ASE spectrum for 3.6 μm, 110 μm mesa width device at 80 K showing notches due to leaky mode loss

The notches shown in Fig. 4 are caused when the waveguide modes are resonant with the substrate modes. In this case, substantial energy can be transferred out of the waveguide into the resonant substrate modes. From the substrate, light can be radiated out of the crystal [9]. Owing to the greater thickness of the substrate as compared to the waveguide, diffraction-limited light from the substrate could form a better collimated beam than light from the waveguide [10].

The experimentally observed mode grouping can be explained by the interference effect of leaky substrate modes [7]. The refractive indexes of the multilayer active region, n_{AR}, and superlattice claddings, n_C, were obtained for this model calculation by averaging the bulk values with respect to the layer widths. The bulk values for binary materials have been taken from Adachi [11], with linear interpolation for alloys. For simplicity, we assume similar dispersion for both n_{AR} and n_C. The width of the narrow top buffer layer is substantially smaller than the lasing wavelength λ, and the corresponding gain modulation period δ will exceed the observed gain spectrum width. It is the reflection from the lower contact and the phase shift gained during the radiation propagation through the thick substrate layer of width $h_S \gg \lambda$, which primarily affect the interference process. We thus assume that the interference of substrate leaky modes dominates the observed pattern of the gain modulation. The influence of the medium gain on the refractive index has been also neglected in this simplified model [12].

Within these approximations, the optical loss due to the substrate leakage α_l and corresponding gain modulation period δ can be expressed as [7]:

$$\alpha_l = \frac{q_S}{\beta' d_{eff}} \cdot \frac{4p_C^2 \cos^2(q_{AR} d_{AR}/2)}{p_c^2 + q_S^2} \cdot \frac{\exp(-2p_C d_{C2})(1 - |R|^2)}{|1 - R \cdot \exp(-i\psi)|^2} \quad (1)$$

$$\delta = \frac{\lambda^2}{2h_S} \cdot \frac{1 + p_C d_{C2}/2}{Q_S} \quad (2)$$

where

$\beta' = (\omega/c)(n_{AR}^2 - Q_{AR}^2)^{1/2}$ is the effective propagation constant along the waveguide axis,
$q_{AR} = (\omega/c)Q_{AR}$ is the effective transverse propagation constant in the active region,
$q_S = (\omega/c)Q_S = (\omega/c)(n_S^2 - n_{AR}^2 + Q_{AR}^2)^{1/2}$ is the transverse propagation constant in the substrate,
$p_C = (\omega/c)P_C = (\omega/c)(n_{AR}^2 - n_C^2 + Q_{AR}^2)^{1/2}$ is the transverse attenuation constant in the claddings,
$R = r\exp(2iq_S h_S)$ is the phase shift due to the round trip through the substrate with r the effective amplitude reflection coefficient from the bottom contact,
$\tan\psi = P_C/Q_S$
and the effective mode width is

$$d_{eff} = \frac{d_{AR}}{2}\left(1 + \frac{\sin(q_{AR}d_{AR})}{q_{AR}d_{AR}}\right) + \frac{\cos^2(q_{AR}d_{AR}/2)}{2p_C} \times [2 - \exp(-2p_C d_{C1}) - \exp(-2p_C d_{C2})] \quad (3)$$

Indexes 1 and 2 above relate to the top and bottom claddings, respectively. The quantity Q_{AR} is to be found from the dispersion equation:

$$\tan\frac{q_{AR}d_{AR}}{2} = \frac{(n_{AR}^2 - n_C^2 - Q_{AR}^2)^{1/2}}{Q_{AR}} \quad (4)$$

For a given structure layout, we arrive at the following parameter values: $n_{AR} = 3.47$ and $n_C = 3.36$.

The effective gain modulation period was a weak function of the wavelength and changed from 0.065 μm to 0.09 μm in the wavelength range 3.0 μm to 4.0 μm. The calculated optical loss spectrum is shown in Fig. 5. At a high value of the amplitude reflection coefficient r ($r = 0.7$ in the Figure), the gain spectrum is characterised by deep and narrow cuts without strong reduction of the overall gain spectrum curve. This agrees well with our observation that the non-resonant losses related to the leaky mode interference are actually small, so that the devices without interference gain modulation demonstrate practically the same gain envelope with a similar value of the low-frequency optical loss.

Since the notch spacing is dependent on the substrate thickness (see (2)), the leaky mode hypothesis can be tested by checking the gain spectrum of similar samples which have been thinned to a different substrate thickness. The top trace in Fig. 4 shows the net gain for a 3.6 μm device with a

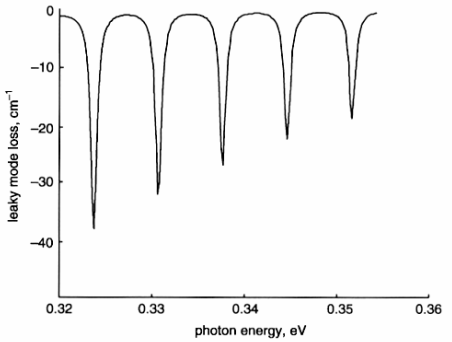

Fig. 5 *Calculated leaky mode loss for device with substrate thickness of 75 μm and substrate reflectivity, r, of 0.7*

130 μm substrate thickness, while the bottom trace is for a device from the same wafer that has been thinned to 75 μm. These devices had different cavity lengths (1 mm for the 130 μm thick sample, 0.5 mm for the 75 μm sample). The simple theoretical model used in this work assumes that the cavity length is much bigger that the substrate thickness. In general, however, any changes in the cavity geometry may lead to changes in notch spacing, especially in the situation when the cavity length and substrate thickness are comparable.

The spacing between the notches is approximately 72 nm for the 75 μm thick sample and approximately 42 nm for the 130 μm device, in agreement with (2). The depth of the notches is also significantly decreased for the 130 μm thick device, possibly due to increased absorption in the thicker substrate, or to a variation in the quality of the substrate surface.

3.2 Gain

Figure 6 is a plot of peak net gain against injection current for one of our devices. At a heatsink temperature of 80 K, the gain is seen to increase linearly with injection current. By extrapolating this curve, it is seen that threshold is reached at an injection current of approximately 10 mA.

At a heatsink temperature of 140 K, the gain curve is markedly different. At the higher temperature the gain is seen to saturate with increasing injection current. This particular gain curve corresponds to operation at just above the device's maximum continuous-wave lasing temperature. Increasing the injection an order of magnitude beyond that shown on this graph still did not bring the laser to threshold.

The devices under consideration here were mounted epi-side up, and are known to have high thermal resistance values, resulting in CW active region temperatures significantly higher than the heatsink temperature [13]. Using low duty cycle pulsed injection, we determined the characteristic temperature T_0 from the temperature dependence of the threshold current density (inset, Fig. 7). The active region temperature, T, could then be estimated by substituting the observed CW threshold current, I, into the model $I = I_0 \exp(T/T_0)$. Figure 7 shows the temperature difference between the active region and the heatsink at threshold as a function of pump current. The rapid increase of the temperature difference is due to the increasing power dissipation in the active region, as higher pump currents are required to achieve threshold at the higher heatsink

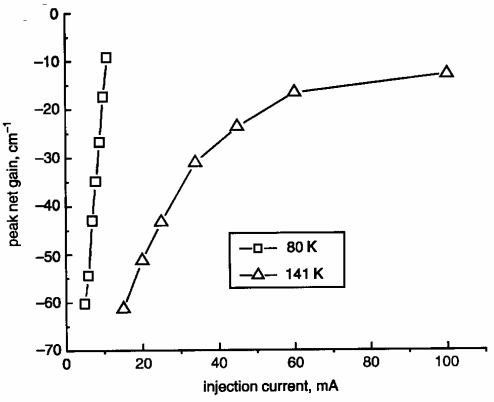

Fig. 6 *Net gain against injection current for a 3.4 μm, 65 μm mesa device at two heatsink temperatures*

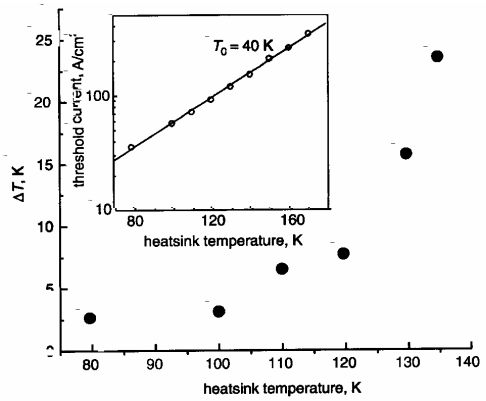

Fig. 7 *Temperature difference between active region and heatsink (ΔT) against heatsink temperature for CW operation of 3.4 μm, 65 μm mesa device at threshold*

Inset: threshold current density against heatsink temperature for 3.4 μm, 65 μm mesa device operated in low duty cycle pulsed mode

temperatures. The positive feedback effect between increasing loss, increasing threshold current and increasing active region temperature limits the maximum operating temperature of these ICLs.

4 Summary

The gain and loss of ICL devices has been measured using the Hakki–Paoli technique. The internal loss was found to increase gradually with temperature. At higher temperatures, the gain saturates before the device reaches threshold. The active region temperature at threshold was found to be significantly higher than the heatsink temperature, and this difference increased rapidly with higher heatsink temperatures.

The longer wavelength samples showed mode grouping effects in their spectra. The mode grouping was shown to be due to mode leakage between the waveguide and the substrate. This leakage can be reduced by increasing the thickness of the cladding layers.

5 Acknowledgments

The authors gratefully acknowledge the contributions made to this work by J. T. Pham (Maxion Technologies, Inc.) and R. Q. Yang (Jet Propulsion Laboratory). Work at SUNY was supported by the MURI, AFOSR Grant F49620-00-1-0331 and the ARO grant DAAD 190010423.

6 References

1 Yang, R.Q.: 'Infrared laser based on intersubband transitions in quantum wells', *Superlattices Microstruct.*, 1995, **17**, (1), pp. 77–83
2 Yang, R.Q., Bradshaw, J.L., Bruno, J.D., Pham, J.T., and Wortman, D.E.: 'Mid-infrared type-II interband cascade lasers', *IEEE J. Quantum Electron.*, 2002, **38**, (6), pp. 559–568
3 Bradshaw, J.L., Pham, J.T., Yang, R.Q., Bruno, J.D., and Wortman, D.E.: 'Enhanced cw performance of the interband cascade laser using improved device fabrication', *IEEE J. Sel. Top. Quantum Electron.*, 2001, **7**, (2), pp. 102–105
4 Vurgaftman, I., Meyer, J.R. and Ram-Mohan, L.R.: 'High-power/low-threshold type-II interband cascade mid-IR lasers – design and modeling', *IEEE Photonics Technol. Lett.*, 1997, **9**, (2), pp. 170–172
5 Hakki, B.W.. and Paoli, T.L.: 'Gain spectra in GaAs double-heterostructure injection lasers', *J. Appl. Phys.*, 1975, **46**, (8), pp. 1299–1306
6 Donetsky, D.V., Belenky, G.L., Garbuzov, D.Z., Lee, H., Martinelli, R.U., Taylor, G., Luryi, S., and Connolly, J.C.: 'Direct measurements of heterobarrier leakage current and modal gain in 2.3 μm double QW p-substrate InGaAsSb/AlGaAsSb broad area lasers', *Electron. Lett.*, 1999, **35**, (4), pp. 298–299

7 Arzhanov, E.V., Bogatov, A.P., Konyaev, V.P., Nikitina, O.P., and Shveikin, V.I.: 'Waveguiding properties of heterolasers based on InGaAs/GaAs strained quantum-well structures and characteristics of their gain spectra', *Quantum Electron.*, 1994, **24**, (7), pp. 581–587
8 O'Reilly, E.P., Onischenko, A.I., Avrutin, E.A., Bhattacharyya, D., and Marsh, J.H.: 'Longitudinal mode grouping in InGaAs/GaAs/AlGaAs quantum dot lasers: origin and means of control', *Electron. Lett.*, 1998, **34**, (21), pp. 2035–2037
9 Summers, H.D., Smowton, P.M., Blood, P., Dineen, M., Perks, R.M., Bour, D.P., and Kneissel, M.: 'Spatially and spectrally resolved measurement of optical loss in InGaN laser structures', *J. Cryst. Growth*, 2001, **230**, pp. 517–521
10 Tilton, M.L., Dente, G.C., Chavez, J., and Gianardi, D.: 'Investigation of substrate modes in InAs/InGaSb W-IA structures'. Proc. 5th Int. Conf. on Mid-infrared optoelectronic materials and devices, MIOMD-V, Annapolis, USA, September 2002, in press
11 Adachi, S.: 'Physical properties of III–V semiconductor compounds' (Wiley, New York, 1992)
12 Ribbat, C., Bognar, S., Sellin, R., and Bimberg, D.: 'Spectral mode dynamics of short cavity quantum-dot lasers', *Appl. Phys. Lett.*, 2002, **81**, (1), pp. 147–149
13 Yang, R.Q., Bradshaw, J.L., Bruno, J.D., Pham, J.T., and Wortman, D.E.: 'Power, efficiency and thermal characteristics of type-II interband cascade lasers', *IEEE J. Quantum Electron.*, 2001, **37**, (2), pp. 282–289